

Development of a Phase Domain Interaction Model of AC and DC Parallel Lines

Tomoatsu Ino Keishi Itachikawa
EEI Department
Kanagawa University
Yokohama, 221-8686, Japan
tino@cc.kanagawa-u.ac.jp

Yoshinori Makino
Electrical Engineering Dept.
EPDC
Tokyo, 104-8165, Japan
yoshi_makino@epdc.co.jp

Yukimasa Maeda
Electric Power Systems Dept.
KCC
Tokyo, 113-8451, Japan
maeda@kcc.co.jp

Abstract - Recently, interaction behavior between AC and DC line, running parallel or crossing, becomes a practical problem to be cleared for better control and protection of both of AC and DC systems. For the demand, the model requires high accuracy for DC initialization and wide range of frequency characteristics. In the paper, we would present a phase domain modeling, resulting model accuracy and the transients behavior of the model.

Keywords: Untransposed Transmission Line, AC-DC Interaction Model, Phase Domain Modeling, DC Initialization

1. INTRODUCTION

The interaction model between AC and DC line, running parallel or crossing, have to capabilities to represent the exact dispersion of the mutual connection between those and accurate DC initialization. The phase domain modeling may be best suit for the modeling because of it's ability representing the unbalance of lines[1-6]. An interaction model in phase domain between a bipole DC and 1 c.c.t. AC transmission line has been published in [7], but the literature of this category is still few. Then we would present the model between a bipole DC line with return wires and 2 c.c.t. AC transmission line. The construction feature of the line may be popular in the populated country.

For the efficient DC initialization and representation in low frequency characteristics, we have proposed a modification of the frequency characteristics in low frequency area[8]. Firstly, we will present the brief illustration on the modification, a technique to achieve accurate fitting in low frequency domain, newly developed approximation method and an evaluation index of the interaction model. Next, the evaluation results on the model fitting and the DC initialization are described. Also, the transient behaviors of the model is presented. Lastly, we conclude that the developed model is adequate for the purpose of interaction analysis.

2. A MODELING IN PHASE DOMAIN

DC and low frequency behavior of the AC-DC interaction model is very important because of the high regulation of the DC current control. Then the special strategies for the modeling are required to achieve accurate low frequency modeling. These strategies are as follows.

2.1 Modification of low frequency characteristics

Even in the low frequency part, surge admittance and attenuation constant has frequency characteristics. The fitting

to the characteristics with formation function always may have error. If the low frequency characteristics can be replaced by a real constant, the fitting may easily land to the real constant and achieve high accuracy.

We have proposed a phase domain modeling in which the model approximation is fitted to the modified frequency characteristics of surge admittance and attenuation in phase domain [8]. The idea is as follows. Suppose that the leakage conductance can be neglected and the frequency is low enough, then the frequency characteristics of the surge admittance Y_{ps} and propagation constant A_p appears as the characteristics of square root of s as described by (1).

$$Y_{ps} \cong \sqrt{CR^{-1}} \cdot \sqrt{s} \quad (1a)$$

$$A_p \cong I - \sqrt{CR} \cdot l \cdot \sqrt{s} \quad (1b)$$

Where I , R , C , l and s are unit matrix, line resistance, line capacitance, line length and Laplace operator respectively. Here, let's replace square root of s to a small positive constant α , as shown by (2a) and (2b), then the pi-equivalent impedance Z_e and admittance Y_e can be derived as (3a) and (3b).

$$Y_{ps} \cong \sqrt{CR^{-1}} \cdot \alpha \quad (2a)$$

$$A_p \cong I - \sqrt{CR} \cdot l \cdot \alpha \quad (2b)$$

$$Z_e = Y_{ps}^{-1} \sinh(\gamma l) \cong R \cdot l \quad (3a)$$

$$\frac{1}{2} Y_e = Y_{ps} \frac{\cosh(\gamma l) - I}{\sinh(\gamma l)} \cong \frac{\alpha^2 l}{2} C \quad (3b)$$

Although square root of s in (1a) and (1b) is replaced to the real constant, still the DC voltage drop and capacitive voltage distribution may be maintained. Here after, We call the frequency characteristics replaced the lower frequency part of original characteristics with (2a) and (2b) as modified frequency characteristics. And the model as modified model.

2.2 A technique to achieve high accuracy in low frequency

Since self-attenuation characteristics in low frequency part is very close to unity such order as 0.999, then the approximated result may exceed unity and become unstable due to slight error of fitting. Therefore the weighting in fitting may be complicated. Then we choose a method to fit to A'_p , shown in (3), instead of A_p . True A_p can be simply obtained through (3).

$$A'_p = I - A_p \quad (3)$$

This choice makes setting of weight simple.

2.3 Fitting methods

Although Linearized Least Square method is widely used for line modeling, it does not always give the optimal fitting. A complimentary fitting may give good fitting in some cases. From above points of view, we developed two optimizing methods as following.

2.3.1 Linearized Least Square Method using real data

The imaginary part of the modified frequency characteristics in 2.1 are already meaningless in low frequency area. Then the fitting method using only real data is desired.

The real part of surge admittance and attenuation characteristics are even function of frequency because these time response are only real. Then, equation (4) is expected to fit these frequency characteristics.

$$W(S) = \frac{a_0 + a_1 S^1 + a_2 S^2 + \dots + a_n S^n}{1 + b_1 S^1 + b_2 S^2 + \dots + b_m S^m} \quad (4)$$

($S = \omega^2$, $m > n$)

Where ω is angular frequency, and the coefficients in (4) can be obtained through Linearized Least Squares method. While, the real part of the stable transfer function set, as shown in (5), can be expressed by (6).

$$F(s) = \sum_i \frac{k_i}{s + p_i} + \sum_j \frac{k_j \omega_{nj}^2}{s^2 + \zeta_j \omega_{nj} s + \omega_{nj}^2} + \sum_l \frac{k_l \zeta_l \omega_{nl} s}{s^2 + \zeta_l \omega_{nl} s + \omega_{nl}^2} \quad (5)$$

Here s is Laplace operator.

$$\text{Real}\{F(s)\} = \sum_i \frac{k_i p_i}{s^2 + p_i^2} + \sum_j \frac{k_j (\omega_{nj}^4 - \omega_{nj}^2 s)}{s^2 + (\zeta_j^2 - 2) \omega_{nj}^2 s + \omega_{nj}^4} + \sum_l \frac{k_l \zeta_l^2 \omega_{nl}^2 s}{s^2 + (\zeta_l^2 - 2) \omega_{nl}^2 s + \omega_{nl}^4} \quad (6)$$

Where S is the same as (4). Here, equation (6) is the decomposition form of (4). Then, the fitting results with (4) is easily transferred to the form of (5) by comparing (5) and equation (6).

2.3.2 Parameter scanning type of fitting

As a complimentary fitting of 2.3.1, A parameter scanning type of optimal fitting was prepared for the formation functions shown in (7a) and (7b).

$$f_1(s) = k_c \left(\frac{1}{1 + s(T_o / \lambda)} - \frac{1}{1 + s(\lambda T_o)} \right) \quad (7a)$$

$$f_2(s) = \frac{k \zeta \omega_n s}{s^2 + \zeta \omega_n s + \omega_n^2} \quad (7b)$$

Scanning parameters for (7a) are k_c , T_o and λ , and for (7b) k , ζ and ω_n . These parameters may be bounded in limited range of value through the frequency-amplitude pattern analysis. The bounded range of each parameter is digitized with logarithmically regular interval. All the digitized

values are tested with fitting error and then one of those which gives minimum fitting error is selected as the optimal parameter. Cascade scanning process with different interval gave efficient fitting. The simple error index, as shown in (8) is used for evaluation of optimal fitting.

$$\text{error} = \frac{1}{N} \sum_{i=1}^N \frac{|r'_i - r_i|}{|r_i|} \quad (8)$$

Where r_i is the real part of the original frequency characteristics, and r'_i is it of fitting results.

For the given frequency span, usually 2 to 3 decades once, both method described in 2.3.1 and 2.3.2 are applied to the fitting. Then the one with smaller error index in (8) is selected in each frequency span.

2.4 Evaluation index of the interaction model

Fitting accuracy and transient calculation time are trade off because the higher fitting accuracy requires the more terms of formation function. Then a proper index for the evaluation of a model is desired. Supposed that the ratio of fitting accuracy to the deviation among each elements of the original mutual frequency characteristics between circuits is close to unity, the modal is inadequate as an interaction model. Then we choose a factor G , shown in (9), as an index of the model evaluation.

$$G = \sum_i \sum_j D_{ij} / \sum_i \sum_j E_{ij} \quad (9)$$

Where D_{ij} is relative standard deviation and expressed by (10). Here g_{ij} is the component of the original frequency characteristics and \bar{g}_{ij} is the mean value among those. E_{ij} is the r.m.s. fitting error.

$$D_{ij} = \sqrt{\frac{1}{N} \sum_{k=1}^N \frac{|g_{ij}(\omega_k) - \bar{g}_{ij}(\omega_k)|^2}{|\bar{g}_{ij}(\omega_k)|^2}} \quad (10)$$

Then, the greater G more than unity implies that the fitting error of each component is small as it is compared to the deviation among components.

3. EVALUATION OF AN INTERACTION MODEL

The configuration of a model line is shown in Fig.9, the model line is based on Hokkaido-Honshu DC link. The AC line is 275 kV and the DC line is ± 250 kV.

3.1 Evaluation of fitting

Phase domain attenuation characteristics and surge

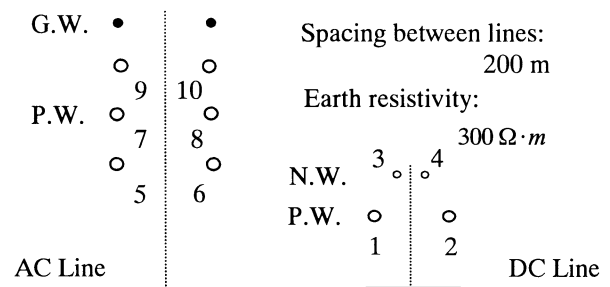


Fig.1. Configuration of a model line.

admittances may be obtained by converting those of the modal domain into the phase domain. Some of eigen values were close each other in the order of 10^{-6} , in the expression in equation (11). But the eigen vector calculation was done as a

$$k = |\lambda_i - \lambda_j| / |\lambda_i| \quad (11)$$

separate eigen value case. Inverse transformation error for YZ was 10^{-5} in maxima and less than 10^{-10} in most frequency points.

In Fig.2a and 2b, the original, modified and fitted real part of attenuation characteristics are shown in the absolute value. In the case, α in (2a) and (2b) is about 0.25, correspondent to 0.01Hz. Fig.2a is an example of the self attenuation in the DC line. The fitting results agree well with

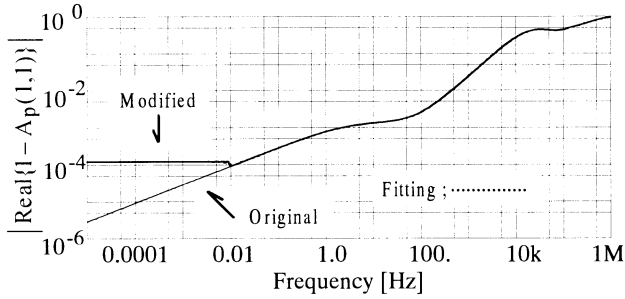


Fig.2a. An example of the self attenuation characteristics in DC line.

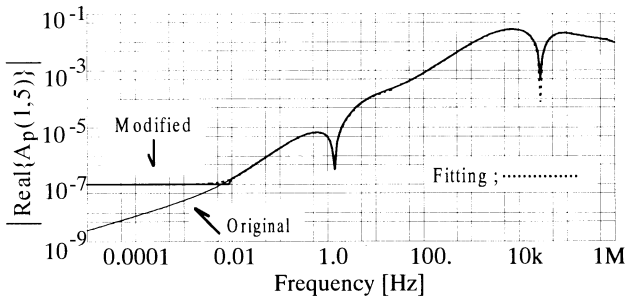


Fig.2b. An example of the mutual attenuation characteristics between AC and DC line.

the original line in the frequency range more than 0.01Hz and the modified line in the range less than 0.01Hz. Also, the fitting makes smooth landing from original frequency characteristics to modified part. Fig.2b is for a mutual attenuation characteristics between AC and DC line. The same conclusion as for the self attenuation can be said.

Fig.3a shows a self surge admittance in DC line. The fitting results agree well with the original and the modified characteristics. The mutual surge admittance between AC and DC line is shown in Fig.3b. The fitting results agree well with the original line in the frequency range more than 0.01Hz and the modified characteristics less than 0.01Hz. But a considerable fitting error is observed by 0.01Hz, because of the jump from original frequency characteristics to the modified one. The square root characteristics of the mutual surge admittance between AC and DC line appears in lower frequency area than that of self or mutual surge admittance in DC or AC line itself. Then the jump may be reduced when a smaller α is selected. But the treatment requires more formation functions. The influence of the jump will be

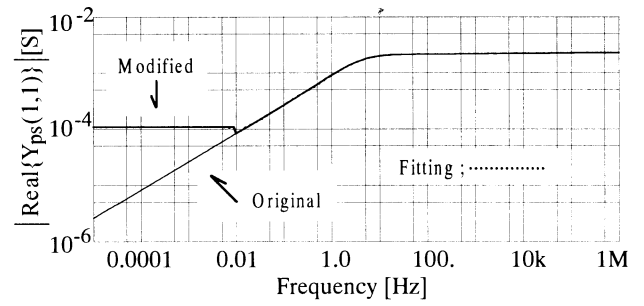


Fig.3a. An example of the self surge admittance in DC line.

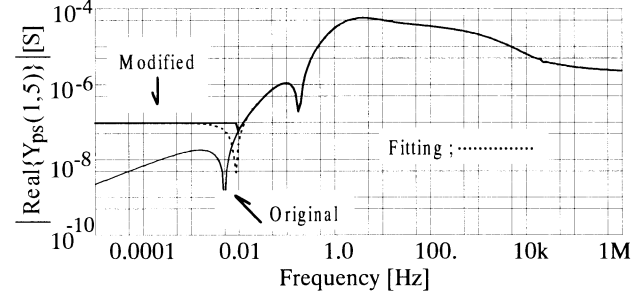


Fig.3b. An example of the mutual surge admittance between AC and DC line.

inspected later in the dynamic behavior.

For the mutual attenuation characteristics between AC and DC line, the factor G in (10) was 33 in the frequency range 0.1 to 100kHz. For the surge admittance, G was 27 in the same frequency range. Then it is considered that the model adequately express the dispersion of the mutual connection between AC and DC.

3.2 DC initialization tests

The following tests were done by using EMTP(DCG V2.1) enhanced with the phase model. The model circuit for a DC current initialization test is shown in Fig.4. The receiving-end voltage V_R was set to 250kV, the sending-end voltage V_S to 250kV plus resistive voltage drop of the DC current 1200A. The maximum current error of DC power conductors was less than 0.13%, equivalent to 1.56 degree

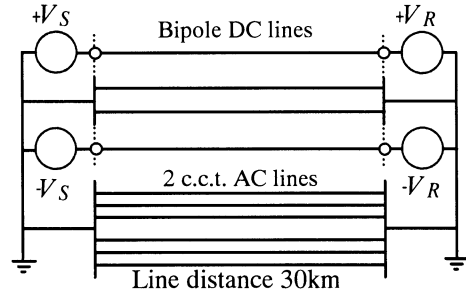


Fig.4. The model circuit for DC initialization test.

deviation of the firing angle, where the current regulation was assumed 1.2k degree per 1p.u. of the DC current. In this case, the currents of other conductors should be theoretically zero. Here, the maximum current of the EMTP code outputs of the other conductors was 0.00082% in the ratio to the 1200A DC current.

Figure 5 shows the model circuit for a DC voltage distribution test. The sending-end of the power conductor 1

of the DC circuit was set to 1 p.u. voltage. Fig.6 shows the voltage distribution during the transient calculation after the

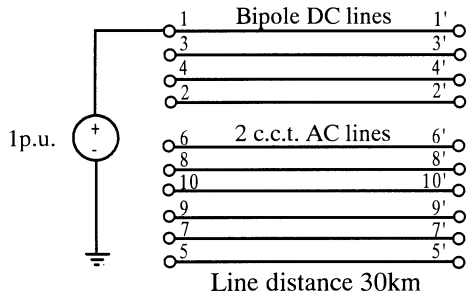


Fig.5. The model circuit for DC voltage distribution test.

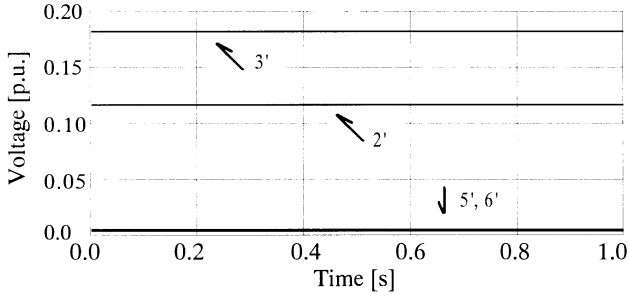


Fig.6. Voltage response during transient calculation after the voltage initialization.

voltage initialization was done at $t=0$. The conductor 2 and 3 belong to the DC circuit and the conductor 5 and 6 to the AC circuits. The voltage distribution reflects capacitive voltage distribution and is stable for 1 second run.

4. TRANSIENT BEHAVIOR OF THE INTERACTION MODEL

In order to examine the effect of the modified frequency characteristics on the transient behavior, the model may be compared with a more accurate model in low frequency band as a reference. Then a reference model, fitted to the original frequency characteristics to 0.0001Hz in lower frequency side, was prepared. Fig.7a and 7b show the fitting results to the mutual attenuation and surge admittance of the reference model. The agreement between those of the fitting and original is well. Also a nominal pi-model can be used as a reference of the steady state in the specific frequency.

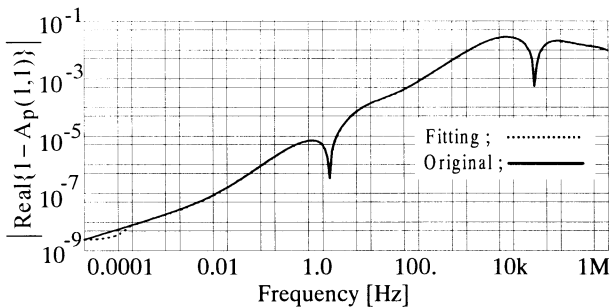


Fig.7a. An example of the mutual attenuation characteristics between AC and DC line.

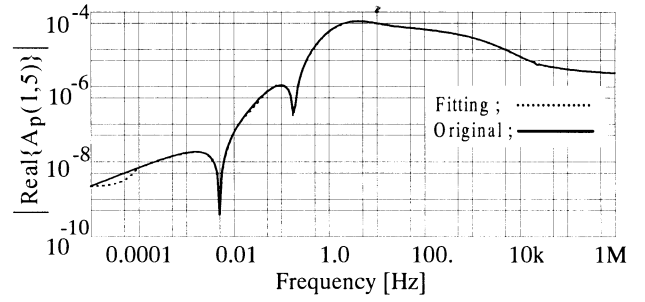


Fig.7b. An example of the mutual surge admittance between AC and DC line.

4.1 Step energizing on DC circuit

The circuit for the step energizing is shown in fig.8. The conductor 1 of the DC circuit is energized at the sending-end with 1 p.u. voltage and the other terminals of conductors remain open. Fig.9a and 9b compare the voltage responses of the modified model on the receiving-end with those of the reference model. Fig.9a shows the transient state and the wider range behavior from transient to steady is shown in fig9b. The wave form of each response of the modified model agrees well with those of the reference model.

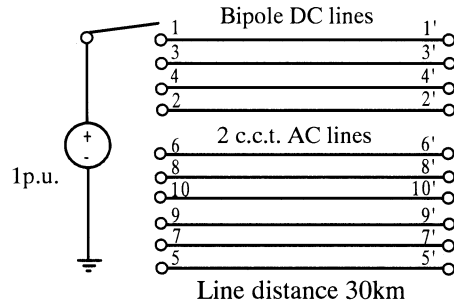


Fig.8. The model circuit for the voltage response test.

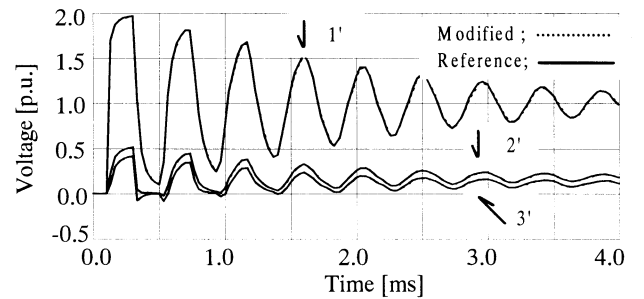


Fig.9a. Step voltage responses of the reference and the modified model (short range).

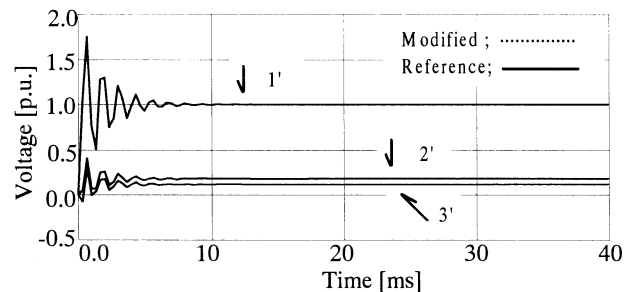


Fig.9b. Step voltage responses of the reference and the modified model (wider range).

The circuit for the current response is shown in fig.10. The step voltage is applied at the sending-end of DC power conductor 1 and the other ends of conductors are connected ground. Fig.11 shows the current responses on the receiving-end of the conductor 1, 2 and 5. Both responses of the modified and reference model agree well each other.

From the above two tests, it may be said that the modified frequency characteristics does not give significant effect in the dynamic behavior.

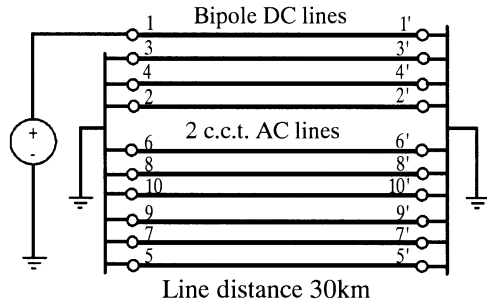


Fig.10. The model circuit for the current response test.

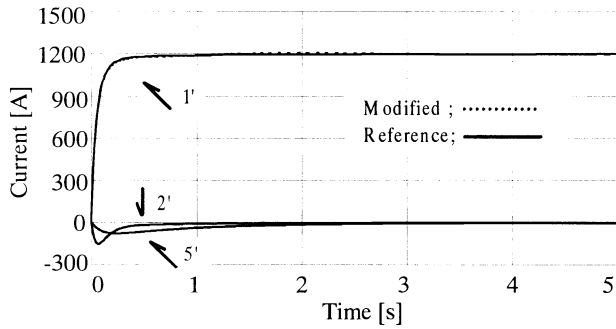


Fig.11. Current responses of the reference and the modified model.

4.2 Power frequency energizing tests of AC circuit

Fig.12 shows the circuit for the test. The sending-end of a AC circuit near by DC side is energized with the voltage source of 50Hz power frequency, equivalent to the voltage drop by normal load current. The other terminals of conductors are grounded except the receiving end of the DC circuit. Then the induced voltages on the receiving end of DC circuit are examined.

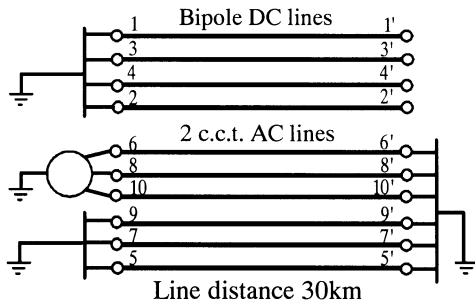


Fig.12. Power frequency energizing tests.

Fig.13a show the transient state of the induced voltage on the DC power conductor 1 produced by the 50Hz nominal pi-

model. The same voltage produced by the modified phase model is shown in fig.13b. The wave form of the pi-model is significantly oscillatory as compared to it of the modified phase model. This is understood as the pi-model gives good solution in only 50Hz steady state. After reaching to the steady state, both waves agreed well each other in the magnitude and the phase. Fig.13c shows the open loop voltage along the DC power conductor 1 and 2. The agreement of the modified phase model and pi-model output is well.

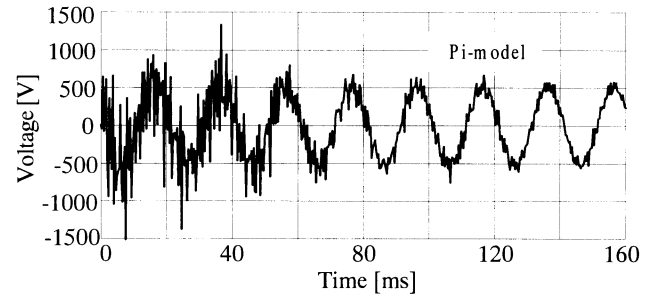


Fig.13a Induced voltage produced by the pi-model.

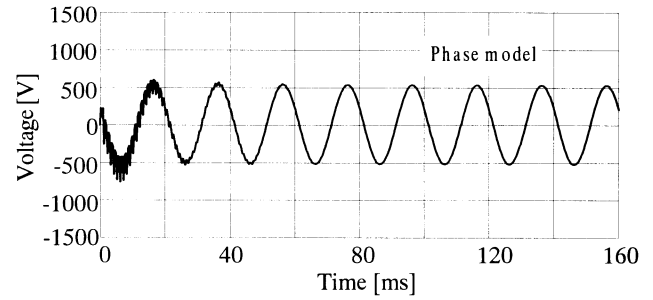


Fig.13b Induced voltage produced by the phase model.

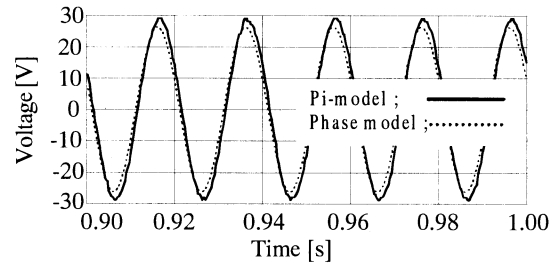


Fig.13c Open loop voltage along DC power conductors.

5. CONCLUSION

A phase domain modeling of the interaction between DC and AC lines was introduced. From the examination of the model fitting, DC initialization and dynamic behavior, the following may be concluded.

- (1) The modeling adequately represent the dispersion of the mutual connection between DC and AC transmission line.
- (2) The modification of the frequency characteristics in low frequency domain gives accurate DC initialization and does not give significant effect in the slow transient.

- (3) In the power frequency, the steady state output of the model agrees well with the pi-model.

6. REFERENCES

- 1] T. Ino, C. Uenosono, "An approximation method of frequency dependent effect in phase frame for unbalanced transmission line.", T. IEE Japan, vol.113B, No. 12, December 1993.
- [2] G. Angelidis, A. Semlyen, "Direct phase domain calculation of transmission line transients using two-sided recursions", IEEE Trans. on Power Delivery, Vol.10, No.2, April 1995
- [3] T. Noda, N. Nagaoka, A. Ametani, "Phase domain modeling of frequency dependent transmission lines by means of ARMA model.", IEEE Winter Meeting, 95 WM 245-1PWRD, January 11, 1995.
- [4] T. Ino, C. Uenosono, "An examination of a phase frame modelling for transients of unbalanced transmission lines with Bergeron method.", T. IEE Japan, Vol.115B, No.9, September, 1995.
- [5] B. Gustavsen, A. Semlyen, "Simulation of transmission line transients using vector fitting and modal decomposition.", IEEE Trans. on Power Delivery, Vol.13, No.2, April 1998.
- [6] B. Gustavsen, A. Semlyen, "Calculation of transmission line transients using polar decomposition.", IEEE Trans. on Power Delivery, Vol.13, No.3, July 1998.
- [7] B. Gustavsen, G. Irwin, R. Mangelrod, D. Brandt, K. Kent, "Transmission line models for the simulation of interaction phenomena between parallel AC and DC overhead lines.", IPST'99, 1999, Budapest Hungary
- [8] T. Ino, M. Sekita, J. Sawada, "An examination of a phase domain modeling of untransposed transmission lines.", IPST'99, 1999, Budapest Hungary